Modeling the radiation pattern of LEDs

Ivan Moreno[1] and Ching-Cherng Sun[2]

[1]*Unidad Academica de Fisica, Universidad Autonoma de Zacatecas, Zacatecas 98060, Mexico*
[2]*Department of Optics and Photonics, National Central University, Tao-Yuan, 320, Taiwan*
imoreno@planck.reduaz.mx, *ccsun@dop.ncu.edu.tw*

Abstract: Light-emitting diodes (LEDs) come in many varieties and with a wide range of radiation patterns. We propose a general, simple but accurate analytic representation for the radiation pattern of the light emitted from an LED. To accurately render both the angular intensity distribution and the irradiance spatial pattern, a simple phenomenological model takes into account the emitting surfaces (chip, chip array, or phosphor surface), and the light redirected by both the reflecting cup and the encapsulating lens. Mathematically, the pattern is described as the sum of a maximum of two or three Gaussian or cosine-power functions. The resulting equation is widely applicable for any kind of LED of practical interest. We accurately model a wide variety of radiation patterns from several world-class manufacturers.

OCIS codes: (230.3670) Light emitting diodes; (220.4830) Optical system design; (350.4600) Optical engineering; (120.5630) Radiometry; (150.2950) Illumination.

References and links

1. E. F. Schubert, J. K. Kim, "Solid-state light sources getting smart," Science **308**, 1274-1278 (2005).
2. Y. Narukawa, "White-light LEDs," Opt. Photon. News **15**, 24–29 (2004).
3. A. Zukauskas, M. S. Schur, R. Gaska, *Introduction to Solid State Lighting* (Wiley-Interscience, NY, 2002).
4. M. S. Kaminski, K. J. Garcia, M. A. Stevenson, M. Frate, and R. J. Koshel, "Advanced Topics in Source Modeling," Proc. SPIE **4775**, 46 (2002).
5. H. Zerfhau-Dreihöfer, U. Haack, T. Weber, and D.Wendt, "Light source modeling for automotive lighting devices," Proc. SPIE **4775**, 58 (2002).
6. M. Jongewaard, "Guide to selecting the appropriate type of light source model," Proc. SPIE **4775**, 86-98 (2002).
7. W. J. Cassarly, "LED modelling: pros and cons of common methods," Photon. Tech Briefs IIa-2a (April 2002), special supplement to NASA Tech Briefs.
8. P. Benitez, J. C. Miñano, "The Future of illumination design," Optics & Photonics News **18**, 20-25 (2007).
9. M. W. Siegel, R. D. Stock, "General near-zone light source model and its application to computer-automated reflector design," Opt. Eng. **35**, 2661-2679 (1996).
10. R. D. Stock, M. W. Siegel, "Orientation invariant light source parameters," Opt. Eng. **35**, 2651 (1996).
11. I. Ashdown, "Near-field photometry: a new approach," J. Illum. Eng. Soc. **22**, 163-180 (1993).
12. I. Moreno, "Spatial distribution of LED radiation," Proc. SPIE **6342**, 634216 (2006).
13. P. Manninen, J. Hovila, P. Kärhä, E. Ikonen, "Method for analysing luminous intensity of light-emitting diodes," Meas. Sci. Technol. **18**, 223-229 (2007).
14. C. C. Sun, T. X. Lee, S. H. Ma, Y. L. Lee, S.M Huang, "Precise optical modeling for LED lighting verified by cross correlation in the midfield region," Opt. Lett. **31**, 2193-2195 (2006).
15. W. T. Chien, C. C. Sun, I. Moreno, "Precise optical model of multi-chip white LEDs," Opt. Express **15**, 7572-7577 (2007).
16. Application brief AB20-5, "Secondary Optics Design Considerations for SuperFlux LEDs" Philips Lumileds.
17. E. F. Schubert, J. K. Kim, H. Luo, J. Q. Xi, "Solid-state lighting—a benevolent technology," Rep. Prog. Phys. **69**, 3069–3099 (2006).
18. C. C. Sun, C. Y. Lin, T. X. Lee, T. H. Yang, "Enhancement of light extraction of GaN-based light-emitting diodes with a microstructure array," Opt. Eng. **43**, 1700-1701 (2004).
19. A. Estrada-Hernandez, L. P. Gonzalez-Galvan, H. Zarate-Hernandez, R. Cardoso, E. Rosas, "Luminous flux and correlated color temperature determination for LED sources," SPIE **6422**, 64220O (2007).
20. R. Young, "Measuring light emission from LEDs," SPIE **6355**, 63550H (2006).

#90469 - $15.00 USD Received 3 Dec 2007; revised 20 Jan 2008; accepted 21 Jan 2008; published 25 Jan 2008

21. C. Daniel, F. S. Wood, *Fitting equations to data: computer analysis of multifactor data* (2nd ed.), (Wiley, New York, 1999).
22. L. Fu, R. Leutz, H. Ries, "Physical modeling of filament light sources," J. Appl. Phys. **100**, 103528 (2006).
23. J. Arasa, S. Royo, C. Pizarro, J. Martinez, "Flux spatial emission obtained from technical specifications for a general filament light source," Appl. Opt. **38**, 7009-7017 (1999).
24. D. R. Jenkins, H. Monch,, "Source Imaging Goniometer Method of Light Source Characterization for Accurate Projection System Design," SID Symposium Digest **31**, 862-865 (2000).
25. S. Preuss, D. Potthoff, T. Preuss, K. Lischka, "LED encapsulation- a new approach of rear light design," SPIE **6198**, 61980I (2006).
26. S. C. Allen, A. J. Steckl, "ELiXIR—Solid-State Luminaire With Enhanced Light Extraction by Internal Reflection," J. Display Technol. **3**, 155-159 (2007).
27. I. Moreno, U. Contreras, "Color distribution of multicolor LED arrays," Opt. Express **15**, 3607-3618 (2007).
28. I. Moreno, M. Avendaño-Alejo, R. I. Tzonchev, "Designing light-emitting diode arrays for uniform near-field irradiance," Appl. Opt. **45**, 2265–2272 (2006).
29. S. Tryka, "Radiative flux from a planar multiple point source within a cylindrical enclosure reaching a coaxial circular plane," Opt. Express **15**, 3777-3790 (2007)
30. S. Tryka, "Spherical object in radiation field from a point source," Opt. Express **12**, 512-517 (2004).
31. J. L. Balenzategui, A. Marti, "Design of hemispherical cavities for LED-based illumination devices," Appl. Phys. B **82**, 75-80 (2006).
32. A. L. Dubovikov, S. S. Repin, S. N. Natarovskii, "Features of the use of LEDs in artificial-vision systems," J. Opt. Technol. **72**, 40-42 (2005).
33. T. Matsumoto, N. Inoue, M. Suzuki, "Optimum arrangement of LEDs in base station of optical wireless LANs," SPIE **6134**, 613403 (2006).
34. C. G. Lee, C. S. Park, J. H. Kim, D. H. Kim, "Experimental verification of optical wireless communication link using high-brightness illumination light-emitting diodes," Opt. Eng. **46**, 125005 (2007).
35. J. M. Kahn and J. R. Barry, "Wireless infrared communications," Proc. IEEE **85**, 265-298 (1997).
36. D. W. K. Wong, G. Chen, "Illumination design of a white-light-emitting diode wireless transmission system," Opt. Eng. **46**, 085002 (2007).
37. M. Akanegawa, Y. Tanaka, M. Nakagawa, "Basic study on traffic information system using LED traffic lights," IEEE Transactions on Intelligent Transportation Systems **2**, 197-203 (2001).
38. I. Moreno, J. Muñoz, R. Ivanov, "Uniform illumination of distant targets using a spherical light-emitting diode array," Opt. Eng. **46**, 033001 (2007).
39. I. Moreno, "Color tunable hybrid lamp: LED-incandescent and LED-fluorescent," SPIE **6422**, 64220N (2007).
40. Y. Tu, S. Jin, Y. Wang, L. Dou, "Color uniformity and data simulation in High-Power RGB LED modules using different LED-chips arrays," SPIE **6828,** 682816 (2007).
41. C. Deller, G. Smith, J. Franklin, "Colour mixing LEDs with short microsphere doped acrylic rods," Opt. Express **12**, 3327-3333 (2004).
42. C. A. Deller, J. B. Franklin, G. B. Smith, "Lighting simulations using smoothed LED profiles compared with measured profiles," SPIE **6337**, 63370X (2006).
43. M. A. Volkova, S. V. Zlatina, S. N. Natarovskii, O. N. Nemkova, T. F. Selezneva, N. B. Skobeleva, D. N. Frolov, L. M. Kogan, and B. P. Papchenko, "Prospects of using LEDs in the illuminating systems of microscopes," J. Opt. Technol. **72**, 186-190 (2005).
44. C. Ye, Y. Liu, F. Yu, "New Illumination Patterns in Microscopes" SPIE **6033**, 60330L (2005).
45. J. Xu, Z. Xiao, T. Lin, "The Design of Microscope Field Illumination System Based on LED" SPIE **6841**, 68410U (2007).
46. C. C. Sun, I. Moreno, S. H. Chung , W. T. Chien, C. T. Hsieh, T. H. Yang, "Brightness management in a direct LED backlight for LCD TVs," J. Soc. Inf. Disp. In press (2007).
47. G. Harbers, S. J. Bierhuizen, M. R. Krames, "Performance of high power light emitting diodes in display illumination applications" J. Display Technol. **3**, 98-109 (2007).
48. J. W. Whang, Y. T. Teng, "Uniform illumination system with desired emitting angle," SID Conf. Rec. Int. Display Res. Conf., 100-103 (2006).
49. Y. Uchida, T. Taguchi, "Lighting theory and luminous characteristics of white light-emitting diodes," Opt. Eng. **44**, 124003 (2005).
50. L. Svilainis, V. Dumbrava, "LED Far Field Pattern Approximation Performance Study," *Information Technology Interfaces, 2007. ITI 2007. 29th International Conference on*, 645-649 (2007).
51. M. Bennahmias, E. Arik, K. Yu, D. Voloshenko, K. Chua, R. Pradhan, T. Forrester, T. Jannson, "Modeling of non-Lambertian sources in lighting applications," SPIE **6669**, 66691A (2007).
52. A. L. Fischer, "LEDs and displays: Analytical method for computing color patterns in LEDs," Photonics Spectra **41**, 87-88 (June 2007).
53. K. Man, I. Ashdown, "Accurate colorimetric feedback for RGB LED clusters," SPIE **6337**, 633702 (2006).

#90469 - $15.00 USD Received 3 Dec 2007; revised 20 Jan 2008; accepted 21 Jan 2008; published 25 Jan 2008

1. Introduction

Today, LEDs are everywhere, in many shapes and forms, and cover a wide range of applications from indicator lights to solid-state lighting. They are gradually taking over traditional radiation sources because of their attractive characteristics [1-3]. The need for realistic lighting designs is growing, but LEDs are far more difficult to model than the conventional sources. This is worsened because there is a wide variety of LED radiation patterns.

A radiation pattern describes the relative light strength in any direction from the light source. Several approaches are used to model this in real light sources. The models currently employed can be classified as analytical approximations or Monte Carlo ray tracing [4-7]. A ray tracing model is very useful when analyzing and designing the package and the secondary optics for the source. The analytic models are very useful when studying and optimizing the radiation transfer from the source to a target without intermediate complex optics. This is very common with LEDs because they have integrated optics. Secondary optics can also be analytically designed by non-imaging optics methods [8]. Additionally, an analytic equation of the radiation pattern gives researchers and lighting designers more flexibility in analyzing the light in their application.

Radiometric and photometric modeling of a light source can be separated into two classes: near field and far field. In near field a source is modeled as an extended area, and it is usually assumed that the distance to the illuminated target is shorter than 5 times the maximum source dimension [9-11]. A far-field model assumes that the target is farther from the source than this nominal separation, and models the source as an emitting point. However, this rule of thumb is not so easily applied to LEDs because of the radiance complexity and wave effects [12-14]. Then the concept of the mid field was proposed [14], which is similar but not equal to the radiometric near field. The rapid variation of the light pattern in the mid field opens a window for verification of an optical model for a light source like an LED. Using the radiometric definition, a high-power LED with a $1mm^2$ chip should have a 5-mm near field, but in practice up to 20-mm mid fields are found.

In this paper we consider the region after the mid field, i.e. the far field region, where the normalized radiation pattern does not change with the LED-to-target distance. In most cases, the LED's far field began at a short distance. For example, measurements on high-power LEDs (with a $1mm^2$ chip) in our laboratory indicate that this distance (from the tip of the LED) is about 20mm for some power LEDs, and a little longer in multi-chip LEDs [15].

The radiation pattern in far field is characterized by the angular intensity distribution. Radiant (or luminous) intensity is the radiant (or luminous) flux per solid angle in a given direction from the source. In this paper, we realistically model the radiant (or luminous) intensity of LEDs, which is useful in many applications (see Sec. 5).

In what follows, we describe in detail our generalized analytic model. In Section 2, we examine some general properties of an LED radiation pattern, and propose a simple equation that renders the contributions from the emitting region (chip), and the light redirected by the reflecting cup and the encapsulating lens. In Sec. 3, we describe a procedure to fit the model to particular types of LEDs. A radiation pattern gallery for several manufacturer datasheets is presented in Sec. 4, as well as the irradiance calculation. Some typical applications are briefly commented in Sec. 5 and we give our conclusions in Sec. 6.

2. Model development

LEDs are available in many different beam patterns which makes it difficult to find a general model for the multiple LED types. Based on our experience in radiometric theory and ray tracing simulations [12,14,15], we developed a phenomenological model based on light propagation characteristics from its generation inside the chip to its propagation through the packaging lens. Phenomenological models are of utmost importance for real applications in almost all branches of scientific practice, because they relate the real phenomenon to the underlying fundamental theory.

#90469 - $15.00 USD Received 3 Dec 2007; revised 20 Jan 2008; accepted 21 Jan 2008; published 25 Jan 2008

In LEDs, light is produced by spontaneous emission from the light-emitting region of chip. Therefore, the generated light is incoherent and its superposition is a linear combination in intensity terms. From the radiometric point of view, the emitting region is a Lambertian light source. Before exiting the chip, the light generated in this region propagates through different media and types of surfaces. The radiation pattern emitted by every chip face will generally be Lambertian, although in some LEDs, this pattern is modified by special microstructures on the chip and by wave guide effects inside the chip.

The final light pattern generated by an LED is the result of the sum of three terms: the light directly refracted by the encapsulating lens, the light internally reflected inside the lens, and the light reflected by the reflecting cup. These contributions generally are continuous functions that depend on the geometry of both the reflective cup and the encapsulating lens. In other words, the radiation pattern emitted by the chip is modified by the internal reflection inside the encapsulating lens, the reflection in the back mirror, and by the refraction through lens.

In particular, there are three structural factors that strongly modify the radiation pattern of the emitting region [16]. The first is the roughness of the chip faces which causes every chip face to emit a Lambertian pattern (simple cosine function) or a narrow pattern (narrowed by microstructures on the chip and wave guide effects). Physical models of rough surfaces will often result in a surface reflection and transmission consisting of Gaussian and cosine-power functions [17,18]. The second factor is the geometry and roughness of the reflective cup. And, the third, geometry of the encapsulant lens, which distorts the radiation pattern produced by the chip and the reflected by the mirror. Also, due to reflections in the internal surface of the lens, another pattern appears, but is weaker than the others. In most cases, the lens angularly narrows the radiation pattern (due to the chip and the mirror), though sometimes it enlarges the pattern.

Taking into account all the above mentioned phenomena, one could assume that the light pattern is a linear combination of certain Lambertian functions and of some other functions generated by diffuse reflections and diffuse refractions (mainly Gaussian and cosine-power angular functions). From the ray-tracing point of view, every ray of light that is diffusely reflected or refracted spreads in a Gaussian or a cosine-power distribution. Therefore, the final radiation pattern should be a linear superposition of this type of functions, which are angularly shifted in function of the angle of incidence of every traced ray. This function overlapping (in a continuous angular range) in turn generates a single Gaussian or cosine-power function, which is:

$$\int_{\theta 1}^{\theta 2} \exp\left(-b_1(\theta-\alpha)^2\right) d\alpha \cong A\exp\left(-b_2\theta^2\right),$$

and

$$\int_{\theta 1}^{\theta 2} [\cos(\theta-\alpha)]^{m1} d\alpha \cong B\cos^{m2}\theta \quad ,$$

this approximation should surely simplify the resulting radiation pattern.

Thus, taking into account all these criteria, we propose the following general and compact analytical representation of the intensity pattern of LEDs as a sum of Gaussian functions:

$$I(\theta)=\sum_i g1_i \exp\left(-\ln 2\left(\frac{|\theta|-g2_i}{g3_i}\right)^2\right), \tag{1}$$

or as one sum of cosine-power functions:

$$I(\theta)=\sum_i c1_i \cos\left(|\theta|-c2_i\right)^{c3_i} . \tag{2}$$

#90469 - $15.00 USD Received 3 Dec 2007; revised 20 Jan 2008; accepted 21 Jan 2008; published 25 Jan 2008

Here intensity $I(\theta)$ [Arbitrary Units / sr] is defined as the flux emitted per unit solid angle in a given direction. θ is the polar angle in a coordinate system centered in the LED. We choose a one-dimensional equation because most of the LED radiation patterns are rotationally symmetric in far field. Otherwise, we could not do this if some rotational asymmetries in the radiation pattern appear due to emission non-homogeneities on the chip surface and some package obstructions (e.g. wire bondings), which is more significant in the mid field.

Some LEDs show a quite different radiation pattern in two perpendicular azimuthal directions mainly due to a rotationally asymmetric package. In such a case, an appropriate angular variation should be introduced. A useful example with Gaussian functions is:

$$I(\theta,\phi)=\sum_i g1_i \exp\left[-(\ln 2)\left(|\theta|-g2_i\right)^2\left(\frac{\cos^2\phi}{(g3_i)^2}+\frac{\sin^2\phi}{(g4_i)^2}\right)\right], \tag{3}$$

and with cosine-power functions

$$\boldsymbol{I}(\theta,\phi)=\sum_i \boldsymbol{c}1_i \cos\left[|\theta|-\left(\boldsymbol{c}2_i\cos^2\phi+\boldsymbol{c}3_i\sin^2\phi\right)\right]^{\boldsymbol{c}4_i}. \tag{4}$$

where ϕ is the azimuthal angle. Equations (1)-(4) are quite accurate for most LED types, and can be used as a generic LED source model. The radiation pattern can also be represented as a combination of the functions of these equations depending on the type of distribution. In some special cases, one term of the equation can be substituted by two twin terms (see Eq. (8)).

These analytical representations are quite compact. For example, an intensity pattern reproduced with the sum of 2 Gaussian (or cosine power) functions requires about 15 sinusoidal functions to be reproduced with a similar accuracy. Equations (1)-(4) have a number of advantages (see Sec. 5), e.g., they can be used for easily determining derivative values, definite integrals, analytic optimization of LED arrays, etc.

If $I(\theta,\phi)$ is a normalized intensity distribution, the absolute intensity can be computed by measuring the LED flux Φ_0 [19,20], or with the value provided by the manufacturer. The absolute intensity is then:

$$I(\theta,\phi)_A=\left[\frac{\Phi_0}{\int_{4\pi} I(\theta,\phi)d\Omega}\right]I(\theta,\phi). \tag{5}$$

$I(\theta,\phi)_A$ is the radiant intensity [W/sr] if Φ_0 is the radiant flux [Watts], and it is the luminous intensity [lm/sr] when Φ_0 is the luminous flux [lumens].

The sum of Gaussian and cosine-power functions requires nonlinear regression to fit our model to real data. This issue is reviewed in the next section.

3. Numerical fitting

Fitting equations to data is a very common mathematical process in different disciplines of science and technology [21]. The numerical adjustment has been very useful to obtain realistic models for a great variety of light sources in both near and far field regions [9,10,22-24]. Here, we fit a compact analytical representation that optically models LEDs, in particular Eqs. (1)-(4) which are nonlinear in angle.

3.1 Nonlinear regression

A nonlinear regression is an iterative procedure, and the program must start with estimated values for each coefficient. It then adjusts these initial values to improve the fit. Not all mathematical programs are suited to efficiently compute a nonlinear fitting. However, some

#90469 - $15.00 USD Received 3 Dec 2007; revised 20 Jan 2008; accepted 21 Jan 2008; published 25 Jan 2008

software packages provide initial values automatically if a built-in equation is used. Fortunately, a linear sum of Gaussians is commonly a built-in equation. In the case of mixed equations with cosine powers and Gaussians, initial values must be chosen carefully. For example, the initial value of $g2_i$ or $c2_i$ may be that of an intensity peak. It can be useful to estimate initial values after looking at the data graph and understanding the model.

A nonlinear regression program has no common sense. If some problems arise when estimating initial values, it is convenient to set aside the fitting program and continue fitting by trial and error. Depending on the type of radiation pattern, this process can be quickly performed. However, one must think about the optics of the LED, and decide which parameters should be fixed. Then, change the key coefficients one at a time, and see how they influence the shape of the curve and the accuracy of fitting.

3.2 Reconstruction accuracy

To demonstrate the accuracy of reconstruction, the difference between experimental data and modeled equation must be compared by computing both the root mean square (RMS) error and the normalized cross correlation (NCC) [14,15].

The RMS error between experiment (I_e) and modeled equation (I_m) can be calculated on a range of M points over the domain. That is

$$RMS = \sqrt{\frac{1}{M}\sum_i \sum_j \left[I\left(\theta_i, \phi_j\right)_m - I\left(\theta_i, \phi_j\right)_e \right]^2} \,. \tag{6}$$

The reconstructed pattern must be sufficiently accurate, regardless of the type of LED. The RMS error must be less than the standard limit of 5% [21].

Using NCC, the similarity between the simulated pattern (I_m) and the measured pattern (I_e) is

$$NCC = \frac{\sum_i \sum_j \left[I\left(\theta_i, \phi_j\right)_m - \bar{I}_m \right] \left[I\left(\theta_i, \phi_j\right)_e - \bar{I}_e \right]}{\sqrt{\sum_i \sum_j \left[I\left(\theta_i, \phi_j\right)_m - \bar{I}_m \right]^2 \sum_i \sum_j \left[I\left(\theta_i, \phi_j\right)_e - \bar{I}_e \right]^2}} \,, \tag{7}$$

$\bar{I}_m$ and $\bar{I}_e$ are the mean values of simulation and experimental data across the angular range, respectively. From our experience in designing LED lighting systems for industry, we know that an LED model with a NCC higher than 99% gives enough accuracy for many applications [14,15].

3.3 Other details

It is important to know which of Eqs. (1)-(4) should be fitted. This depends on the type of radiation pattern. In particular, cosine-power functions are more suitable than Gaussians when the intensity decreases rapidly with the view angle at the sides of the radiation pattern.

Also, the number of Gaussians or cosine-powers in the equation depends on the type of LED. However, all distributions that we reconstructed (next section) basically required a maximum of 3 terms. This can be linked to the contributions of the three basic optical elements of LEDs: chip, mirror, and lens.

4. LED radiation pattern

Most manufacturers use $\theta_{1/2}$ (the view angle when radiant intensity is half of the value at 0°) to characterize the angular distribution of LEDs with a single intensity peak. This parameter is simply $g3_1$ if Eq. (1) has only one simple Gaussian, e.g. $I(\theta)=g1_1\exp[-\ln 2(\theta/g3_1)^2]$; and this is related to $c3_1$ (i.e., $c3_1=-\ln 2/\ln(\cos\theta_{1/2})$) if Eq. (2) has only one simple cosine power, e.g. $I(\theta)=c1_1[\cos(\theta)]^{c3_1}$. Another attribute used is the total included angle, or θ_{90}, which describes the cone angle within which 90% of the total flux is radiated. However, additional parameters are needed to render the shape of the radiation pattern. Therefore, we propose that the

#90469 - $15.00 USD Received 3 Dec 2007; revised 20 Jan 2008; accepted 21 Jan 2008; published 25 Jan 2008

manufacturer should include a simple formula (like those reported here) with its coefficients in their technical data sheets.

4.1 Intensity distribution tables

Tables of coefficients for equations are very common in optics (e.g. constants for glass dispersion formulas). These tables would be very useful for the scientific and technological communities that use LEDs. This is because LEDs are available in a wide variety of beam patterns, and frequently new beam distributions are reported in academics and industry [25,26].

Figures 1-3 show some modeled radiation patterns of some of the major manufacturers like Nichia, Philips Lumileds, Cree, Edison, Osram, and Seoul Semiconductor. Insets (a), (c), and (e) in Figs. 1-3 are the modeled three-dimensional radiation patterns in polar coordinates (θ,ϕ). A comparison between the modeled angular distribution and the one reported by the manufacturer is shown in the insets (b), (d), and (f) of Figs. 1-3.

Figures 1(a) and 1(b) show the angular distribution of the LED model NSPW345CS from Nichia. This pattern is rotationally asymmetric, so we used Eq. (3), where the XX cross section is for ϕ=0º or 180º, and the XY cross section is for ϕ=90º or 270º. Figures 1(c) and 1(d) show the XLamp® XR-E LED from Cree. This pattern fit better with cosine power functions. And Figs. 1(e) and 1(f) show the LUXEON® Rebel (green, cyan, blue and royal-blue) from Lumileds Philips. Note that switching between the upper bound (UB) and the lower bound (LB) only requires changing the relative intensity coefficients ($g1_1$ y $g1_2$). Because the strength of the two Gaussian terms is linked to the performance of the basic parts of LEDs (chip, mirror, and lens), we can speculate that the variation between the UB and LB is mainly due to manufacturing errors related to the emission, reflection and transmission of the optical flux. In addition, the dependence on only two coefficients for switching between UB and LB makes it easy to simulate manufacturing errors in a system of LEDs with this model.

Figures 2(a) and 2(b) show the angular distribution of the LUXEON® K2 (green, cyan, blue and royal-blue) from Lumileds Philips. Again, the only difference between UB and LB is in the coefficients of the relative intensity $g1_1$, $g1_2$.y $g1_3$. Figures 2(c) and 2(d) show the radiation pattern of a EdiPower™ Emitter 3-RD-01-H0001 LED from Edison. This pattern fits well as a perfect Lambertian emitter, and a first order analysis can be performed by using a simple cosine function, but with a 5.1% RMS error. However, using Eq. (1) with coefficients in Fig. 2(d) improves the analysis accuracy. Figures 2(e) and 2(f) show the distribution of the FIREFLY® Hyper-Bright LB-V19G LED from OSRAM. Its pattern is rotationally asymmetric, thus we used Eq. (4). Only one cosine-power function is required; this fits the pattern better than a Gaussian function because the intensity pattern decreases faster at the sides. The vertical (V) direction is for ϕ=0º or 180º, and the horizontal (H) direction is for ϕ=90º or 270º.

Figures 3(a) and 3(b) show the angular distribution of the LUXEON® Side Emitter from Lumileds Philips (white, green, cyan, blue and royal-blue). We did not simulate the small central peaks because this requires additional Gaussian functions in Eq. (1), and their contribution to NCC and RMS error is insignificant. Figures 3(c) and 3(d) show the radiation pattern of a LUXEON® Batwing from Lumileds Philips (green, cyan, blue and royal-blue). Instead of Eq. (1) we used

$$I(\theta)=g1_1\left[\exp\left(-\ln 2\left(\frac{\theta+g2_1}{g3_1}\right)^2\right)+\exp\left(-\ln 2\left(\frac{\theta-g2_1}{g3_1}\right)^2\right)\right]+g1_2\exp\left(-\ln 2\left(\frac{|\theta|-g2_2}{g3_2}\right)^2\right)$$

$$=h1_1\exp\left[-\ln 2\left(\frac{\theta}{h3_1}\right)^2\right]\cosh\left(h2_1\theta\right)+g1_2\exp\left(-\ln 2\left(\frac{|\theta|-g2_2}{g3_2}\right)^2\right), \quad (8)$$

#90469 - $15.00 USD Received 3 Dec 2007; revised 20 Jan 2008; accepted 21 Jan 2008; published 25 Jan 2008

to fit this pattern because it only requires two terms, avoiding the need of additional functions when using Eqs. (1) or (2). For this pattern, the difference between UB and LB is in almost all the coefficients of Eq. (8). This is in contrast with the recent K2 and Rebel models (Figs. 1(f) and 2(b)), which lead us to believe that the manufacturing quality of Lumileds Philips has been improving over time. Figures 3(e) and 3(f) show the distribution of the Z-Power Side Emitter LED from Seoul Semiconductor. To fit this pattern, we had to displace the entire pattern 2.55º to the right on the radiation angle axis, and then perform the fit. Finally, to plot Fig. 3(f), the resulting Eq. was shifted by 2.55º to the left. This angular deviation of the pattern is probably due to a misalignment of the optical axis of the LEDs tested by the manufacturer.

The advantage of rendering the radiation pattern of a technical data sheet is that the pattern comes from several source samples. Therefore, this angular distribution is representative of that particular LED type. As seen in Figs. 1-3, the rendering accuracy of our model (with respect to manufacturers) is very high; the accuracy threshold, in RMS error and NCC (Sec. 3.2), was surpassed in all cases.

4.2 Irradiance distribution

Irradiance [W/m^2] in far field can be expressed in function of intensity [W/sr]; over a flat surface it is simply:

$$E(r,\theta,\phi)=\frac{I(\theta,\phi)\,\cos\theta}{r^2}, \tag{9}$$

where r is the distance from the source to a target point. Typically, Cartesian coordinates (x,y,z) are used to analyze irradiance over a plane. In such a case, the irradiance of an LED, with an intensity distribution given by Eqs. (1)-(5) or (8), is

$$E(x,y,z)=\frac{z}{\left(x^2+y^2+z^2\right)^{3/2}} I\left[\theta(x,y,z),\phi(x,y)\right] \ , \tag{10}$$

where

$$\theta(x,y,z)=\arctan\left[\frac{\sqrt{x^2+y^2}}{z}\right] \ , \tag{11}$$

$$\phi(x,y)=\arctan\left(\frac{y}{x}\right) \ . \tag{12}$$

If I is the absolute intensity, Eq. (5), then E is the absolute irradiance [W/m^2]. If I is the relative intensity (i.e., Eqs. (1)-(4) and (8)), then E is the relative irradiance [(Arbitrary Units)/m^2]. Equation (10) can be practically used to analyze the irradiance produced by LED arrays, because the relative position of the j-th LED can be taken into account by simply changing coordinates (x,y) by $(x\text{-}x_j,y\text{-}y_j)$ [27,28].

For example, using the UB radiation pattern of a LUXEON® K2 (green, cyan, blue and royal-blue) from Lumileds Philips, $\int I(\theta)d\Omega=4.78$ can be obtained to calculate the absolute irradiance. And with a typical radiant flux Φ_0=575 mW at 1000mA (royal-blue), using Eqs. (5) and (10), the absolute irradiance is

$$E(x,y,z)_{\mathrm{A}}=\frac{120\ z}{\left(x^2+y^2+z^2\right)^{3/2}}\sum_{i=1}^{2} g1_i \exp\left\{-\ln 2\left[\frac{\left|\arctan\left(z^{-1}\sqrt{x^2+y^2}\right)\right|-g2_i}{g3_i}\right]^2\right\}, \tag{13}$$

where E_{A} is in [mW/m^2] if the Cartesian coordinates (x,y,z) are in meters. The coefficients g are those given in Fig. 2(b).

#90469 - $15.00 USD Received 3 Dec 2007; revised 20 Jan 2008; accepted 21 Jan 2008; published 25 Jan 2008

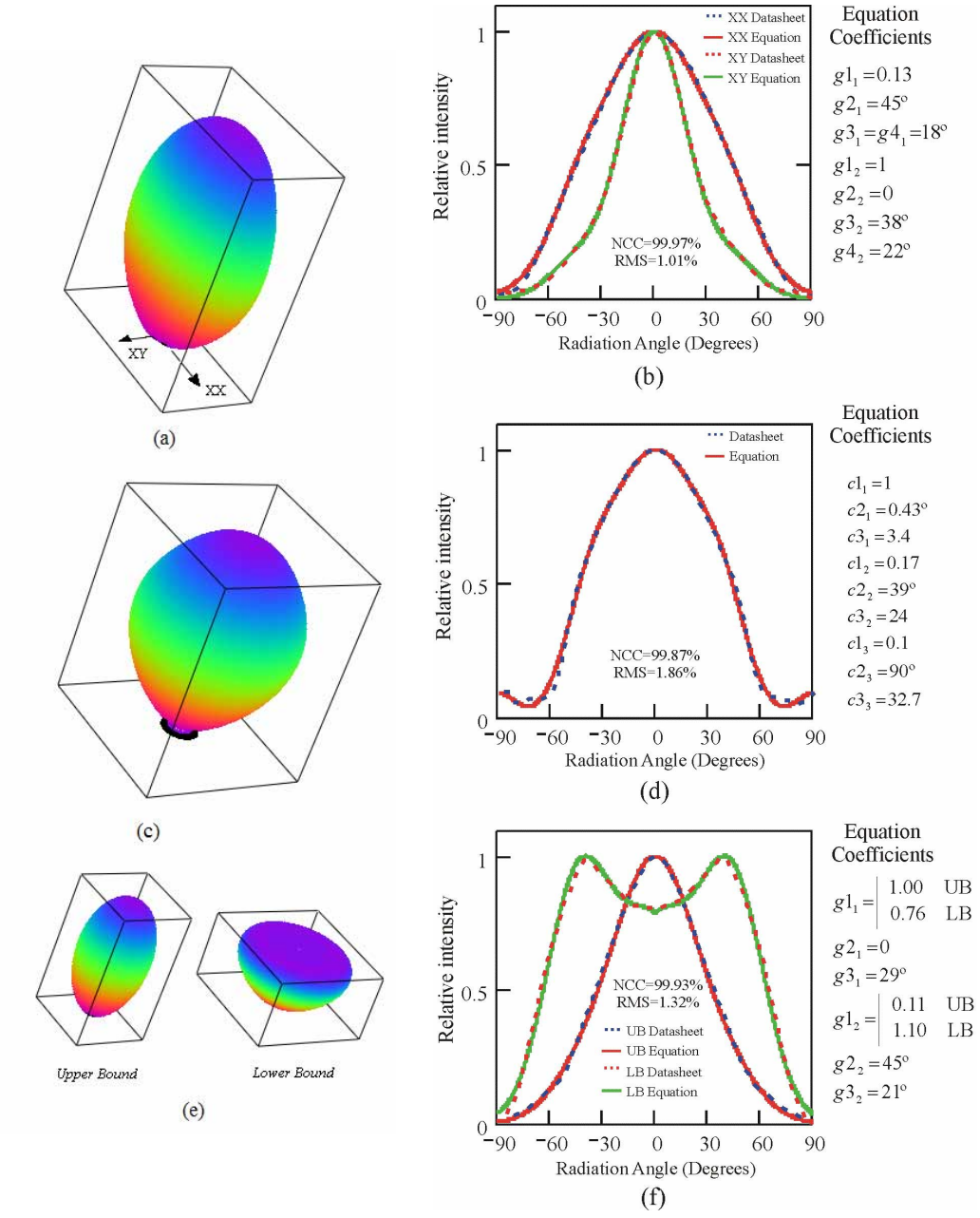

Fig. 1. Three radiation patterns of some major manufacturers. (a) and (b) NSPW345CS from Nichia. (c) and (d) XLamp® XR-E LED from Cree. (e) and (f) LUXEON® Rebel from Lumileds Philips. (a), (c), and (e) are the modeled three-dimensional radiation patterns. (b), (d), and (f) are a comparison between modeled and manufacturer reported radiation pattern. UB-Upper bound, LB-Lower bound, and XX and YY are two perpendicular azimuthal directions.

#90469 - $15.00 USD Received 3 Dec 2007; revised 20 Jan 2008; accepted 21 Jan 2008; published 25 Jan 2008

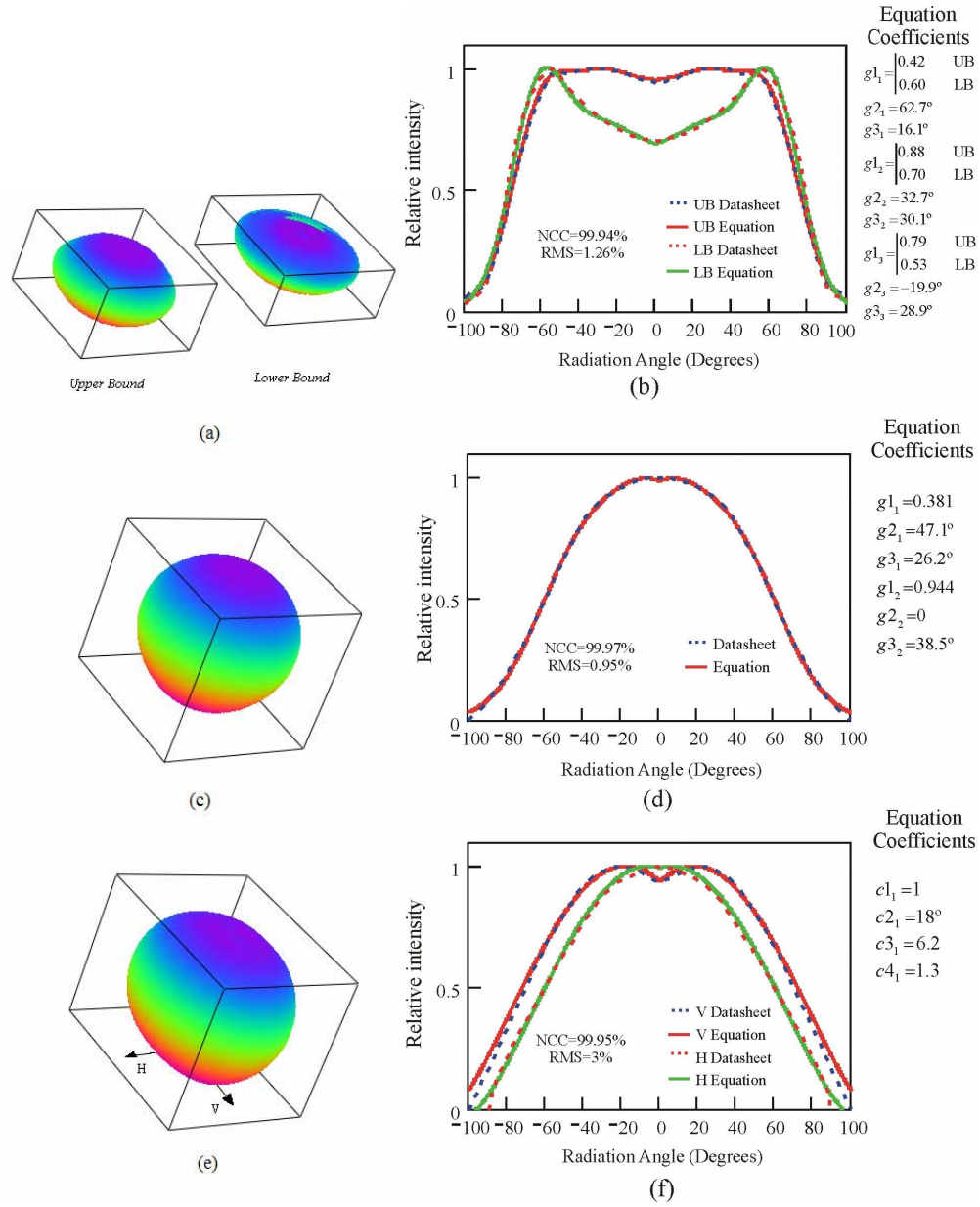

Fig. 2. Other radiation patterns of some major manufacturers. (a) and (b) LUXEON® K2 from Lumileds Philips. (c) and (d) EdiPower™ Emitter 3-RD-01-H0001 LED from Edison. (e) and (f) FIREFLY® Hyper-Bright LB-V19G LED from OSRAM. (a), (c), and (e) are the modeled three-dimensional radiation patterns. (b), (d), and (f) are a comparison between modeled and manufacturer reported radiation pattern. UB-Upper bound, LB-Lower bound, and V and H are the vertical and horizontal directions.

#90469 - $15.00 USD Received 3 Dec 2007; revised 20 Jan 2008; accepted 21 Jan 2008; published 25 Jan 2008

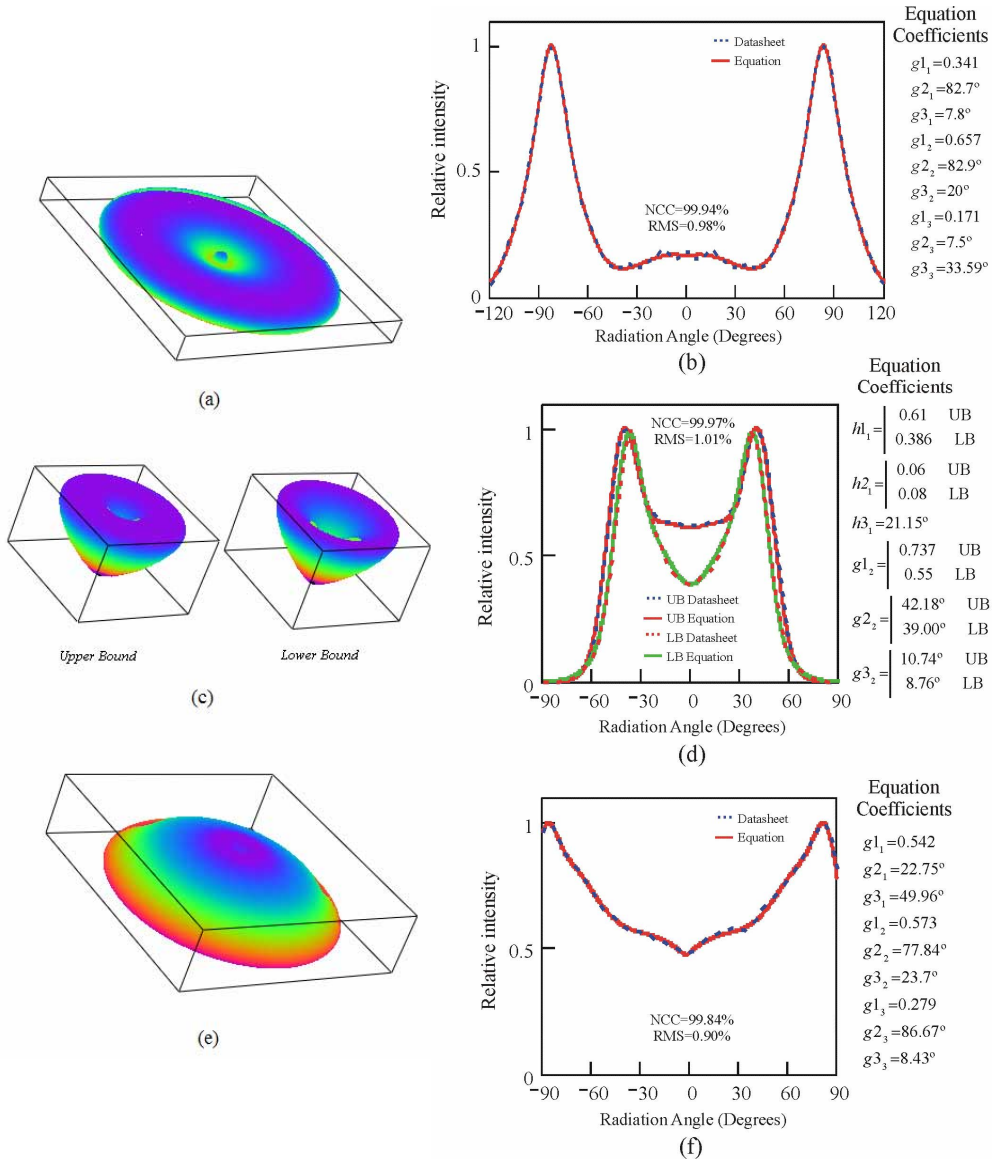

Fig. 3. Other radiation patterns of some major manufacturers. (a) and (b) LUXEON® Side Emitter from Lumileds Philips. (c) and (d) LUXEON® Batwing from Lumileds Philips. (e) and (f) Z-Power Side Emitter LED from Seoul Semiconductor. (a), (c), and (e) are the modeled three-dimensional radiation patterns. (b), (d), and (f) are a comparison between modeled and manufacturer reported radiation pattern. UB-Upper bound, LB-Lower bound.

#90469 - $15.00 USD Received 3 Dec 2007; revised 20 Jan 2008; accepted 21 Jan 2008; published 25 Jan 2008

5. Applications

Analytical far-field approximations (single Gaussian or single cosine power) of the LED radiation pattern have been used in a wide variety of applications [13,28-51]. For example, to determine and optimize the radiation flux reaching detectors, collectors or irradiated targets from arrays of LEDs [29-33]. They are also used in the design of wireless communication systems [33-36], and for using LED traffic lights as transmitters [37]. Analytical functions have been employed in optimizing illumination and color uniformity from LED assemblies in the far and near (with respect to the array size) field [28,38-40]. Also, analytic expressions have been used together with ray trace techniques to design a color mixing device for a multicolor LED assembly [41,42]. Another application is analyzing the LED performance as a light source for a microscope [43-45]. These simple equations are also used in some stages of the optical design of a LED-based backlight for LCD TVs [46-48]. And of course, such equations are used in the design of general illumination systems with white LEDs [49,50].

A single Gaussian or single cosine power is a particular case of our model, as Lambertian (single cosine with $c3_1=1$ and $c2_1=0$), as imperfect Lambertian (single cosine power with $c3_1>1$ and $c2_1=0$) [50,51], or as perfect Gaussian. The imperfect Lambertian and the perfect Gaussian approaches are very similar, and become practically the same pattern for $\theta_{1/2}<30^{\circ}$.

Depending on the accuracy required in simulation, for some applications the uniqueness of individual LED patterns needs to be taken into account [7,41,42,46]. In particular, this is important when the optical system combines the radiation pattern from an array of LEDs. Recently, with our realistic approach, we developed an all analytical method for color pattern determination from multicolor LED arrays [27,52]. Additionally, the intensity pattern of several sample LEDs could be measured to get a set of model coefficients, and then to simulate the optical system by randomly using the model values in the LED array.

6. Conclusion

A simple analytic representation for the radiation pattern of the light emitted from an LED was proposed. The radiation distribution was determined by adding a Gaussian or a power cosine expression for contributions from the emitting surfaces, and the light redirected by both the reflecting cup and the encapsulating lens. To render the intensity distributions, the sum of a maximum of 2 or 3 terms was necessary, which is closely linked to the contributions of the three main parts of LEDs (chip, mirror, and lens). The resulting equation is widely applicable for any kind of LED of practical interest, including Lambertian-type, batwing, and side emitting LEDs. We tested this model against LED datasheets of several major manufacturers, and found that it gives a highly accurate description of the radiation pattern. Moreover, the very simple mathematical representation of the model makes it easy to understand, apply, and perhaps improve it. For example, this model may be useful to introduce random manufacturing variations in the radiation pattern of each LED to realistically design lighting systems consisting of multiple LEDs. Additionally, because the LED emission spectra can be a realistically represented by Gaussian functions, the spectral and spatial distributions may be easily incorporated in a compact analytic representation [53].

Acknowledgments

We thank David Bermúdez and Chang-Yu Tsai for their technical assistance and helpful suggestions. This study was sponsored by the Ministry of Economic Affairs of the Republic of China with the contract no. 94-EC-17-A-07-S1-043. We thank Maureen Sophia Harkins, cetet@uaz.edu.mx, for proofreading this paper.

#90469 - $15.00 USD Received 3 Dec 2007; revised 20 Jan 2008; accepted 21 Jan 2008; published 25 Jan 2008